Spectroscopy and dynamics of the highly excited nonrotating three-dimensional H_3^+ molecular ion

Otto Brass, Jonathan Tennyson,[a] and Eli Pollak

Chemical Physics Department, Weizmann Institute of Science, Rehovot 76100, Israel

A study of the bound states of the H_3^+ molecular ion at zero total angular momentum is presented. Wave functions are shown for the accurate *ab initio* Meyer–Botschwina–Burton potential energy surface and the more approximate diatomics in molecules (DIM) surface. The qualitative behavior is similar for the two potentials. The analytic form of the DIM surface enables a study that reaches energies as high as the dissociation threshold. Quantum states are found to localize regularly around the horseshoe periodic orbits found in previous classical studies. There is good agreement between a semiclassical periodic orbit quantization formula and the exact quantum energies. The antisymmetric stretch frequency with respect to the orbit is estimated classically and quantum mechanically and found to be in agreement with a previous estimate. A three-dimensional stability analysis of the horseshoe orbit is presented and used as a basis for the semiclassical theory. The implications on the assignment of the coarse grained photodissociation spectrum measured by Carrington and Kennedy are discussed.

I. INTRODUCTION

The past few years have seen a significant advance in the experimental determination of spectra of highly excited molecular systems. The stimulated emission pumping technique has opened up a window into the dynamics of highly excited rovibrational states of small polyatomic molecules. Examples are acetylene[1] and the Na_3 cluster.[2] Using a very different method, Carrington and Kennedy have determined, in great detail, the photodissociation spectrum of the H_3^+ molecular ion.[3] The high-resolution UV absorption spectrum of O_3 has also been measured only recently.[4] The common ground of these experiments is that upon coarse graining, the very detailed and seemingly unassignable spectra become quite simple, leading to a small number of frequencies and correlation times.

Because of the complexity and high dimensionality of these molecules, theoretical interpretation has been largely limited to classical trajectory studies. Invariably, one finds a subspace in which classical motion is regular and leads to the correlation times observed in the experiment. Thus, for the Na_3 system, for example,[5] the subspace has two degrees of freedom and the coarse-grained spectrum has been assigned in terms of the modes exhibiting regular motion in the C_{2v} subspace. A detailed classical study of the ozone system has shown that coarse-grained correlation times may be identified with well-defined orbits.[6] The coarse-grained spectrum of H_3^+ has also been interpreted in terms of a two degree of freedom subspace—the family of rotating horseshoe orbits.[7,8]

A quantum theory which bridges between the classical mechanical observations and the experiments has been formulated by Taylor and co-workers.[9] They suggested that the regular classical motion identifies a relatively decoupled region of classical phase space in which one can construct a local basis set. The local basis set defines a P subspace of resonance states, using the Feshbach terminology. The rest of the space serves as a background and the coupling broadens the spectral peaks associated with the resonant states.

The existence of these resonance states has been demonstrated by Taylor and co-workers,[9] using a stabilization method. They found stabilized resonance wave functions, which are localized in the classically decoupled regions. Application to the reduced dimension C_{2v} subspace of H_3^+ clearly showed the horseshoe structure. In a recent paper,[10] we computed all the quantum bound states of C_{2v} H_3^+ and also found strong localization around the horseshoe orbit. Moreover, a semiclassical periodic orbit quantization method[11] accurately predicted all quantum states that localize around the orbit.

These studies were restricted to the two degree of freedom C_{2v} subspace. Extensive three-dimensional (3D) computations for the H_3^+ system have been reported in recent years. Whitnell and Light[12] have used the discrete variable representation (DVR) method[13] to compute converged bound states up to the region of the collinear threshold. Tennyson and Henderson[14] adapted the DVR method in conjunction with an optimized spherical and Morse oscillator basis set and so managed to obtain convergence up to energies well above the collinear threshold. They observed, for the first time, localization around the horseshoe orbit in 3D.

The purpose of the present paper is twofold: (a) to present in more detail the 3D quantum results, paying special attention to localization around the horseshoe mode, and (b) to show that the quantum states localized around the orbit can be assigned and the energies predicted using the periodic orbit quantization method for the full 3D problem.

In Sec. II, we briefly review the elements of the quantal computation and present converged results for two potential energy surfaces. The *ab initio* Meyer–Botschwina–Burton

(MBB) surface[15] is well defined only up to an energy of $\sim 25\,000$ cm^{-1} so that further insight is obtained by studying the states of the less accurate diatomics in molecules (DIM) potential energy surface,[16] which is well defined for all energies.

Application of the periodic orbit quantization method for the full 3D case involves three technical problems which are solved in this paper with novel techniques.

(a) It is necessary to perform a Liapunov stability analysis of the orbit in 3D. In previous attempts, we have encountered difficulties due to numerical instability, when the horseshoe orbit goes through the collinear configuration. Here we removed the instability by performing the analysis in a space-fixed coordinate system. The price to pay is that the dimension of the monodromy matrix to be evaluated is 12×12 instead of the usual 6×6 dimension in the body-fixed frame. The method and the results are described in Sec. III. We find, in agreement with the qualitative conclusions presented in Ref. 8(b), that the stability of the orbit changes with energy. Interestingly, even in the region where the orbit is unstable, one finds quantum states which are localized around it.

(b) The quantum localization around an unstable orbit implies that the orbit is stable in an adiabatic sense, as demonstrated recently in Ref. 17. In the unstable region, it is necessary to estimate the adiabatic stability frequency[18] of the orbit. As described in Sec. III, we find that when the instability of the orbit is not too large, it is possible to obtain a well defined and quantitative estimate of the adiabatic frequency. This is achieved by studying the short time power spectra of trajectories localized around the orbit.

(c) The necessary input for the periodic orbit quantization method is not the Liapunov exponent which is defined mod(2π), but the absolute stability frequency. In a two degree of freedom problem this is relatively easy to obtain.[10,11] The problematics involved in the 3D case and their solution are also described in this section.

All these results are used to assign the quantum states localized along the horseshoe orbit. The implications of this study on our understanding of the coarse-grained photodissociation spectrum of H_3^+ are discussed in Sec. IV.

II. QUANTUM CALCULATIONS

A. Preliminaries

The calculations presented here parallel those of Tennyson and Henderson.[14] Working in Jacobi (or atom–diatom scattering) coordinates, the angular coordinate θ is transformed to a DVR based on Legendre polynomials. The angular terms in the resulting Hamiltonian are diagonal in the potential, but off-diagonal in the kinetic energy. The 3D energies and wave functions were found by first solving the two-dimensional (2D) radial Hamiltonians at each DVR point. The lowest solutions of these reduced problems were then used as a basis to expand the eigenfunctions of the full problem. The radial motions were represented by 23 Morse oscillator-like functions for the r(H–H) coordinate and 31 spherical oscillator functions for the R(H–H$_2$) coordinate. This is the basis we used previously to converge all the bound states in the C_{2v} ($\theta = 90°$) H_3^+ problem.[10] These radial cal-

culations were repeated at the 18 unique DVR points from a DVR based on a 36 point Gauss–Legendre quadrature. Our final calculation used the lowest 2800 of the 12 006 solutions of the radial problems to diagonalize the full Hamiltonian.

Test calculations on the MBB potential[15] showed that this basis is sufficient to converge all the physically significant states of this potential to within 10 cm^{-1}. The convergence for the lower states is much better. Tests on the DIM potential[16] suggested that the convergence is slower. This is in line with our previous observation[10] that the states of this potential are less regular.

The coordinates used in this work do not possess the full symmetry of the H_3^+ system. For zero total angular momentum, the H_3^+ vibrational states occur with A_1, A_2, and E symmetry. In Jacobi coordinates, A_1 and E_e states are symmetric about $\theta = 90°$ and A_2 and E_o states are antisymmetric. In a fully converged calculation it is possible to identify E states by the presence of degeneracies between odd and even symmetry calculations. In this work we also probe high-energy regions for which the computations are not fully converged so that unambiguous assignments are not always possible. For this reason we employ separate numbering schemes for states which result from separately solving the even and odd problems.

B. MBB potential

The MBB potential is an accurate *ab initio* surface for the ground electronic state of the H_3^+ molecular ion. Its main disadvantage is that the fitted form of the potential is well defined only up to $\sim 2/3$ of the dissociation energy into $H_2 + H^+$. The experiments of Carrington and Kennedy are at higher energies, in the vicinity of the dissociation threshold. It is still of interest to study the states of the MBB potential to verify that the results found on the more approximate DIM potential are not a peculiarity of that surface. It is also to be hoped that states of H_3^+ with intermediate energies of 20 000 cm^{-1} will be measured experimentally in the near future.

The eigenvalues of the bound states of the MBB potential for $J = 0$, in the energy range where the surface is well defined, have been given in Table II of Ref. 14. Altogether 180 states were found. Most of the 162 states with energy above the collinear threshold cannot be assigned with any simple zero-order Hamiltonian. The notable exceptions are the states that localize around the horseshoe orbit whose motion is an extreme bending of the proton. The quantum number for this bending motion is therefore denoted as v_2. The symmetric stretching motion with respect to the orbit is designated as v_1, and the antisymmetric stretch as v_3. It should be stressed that although we are using a standard spectroscopic notation, the motion of the horseshoe orbit has a large amplitude and the usual normal mode coordinates appropriate for the low-energy states do not give a good description of the "horseshoe modes."

In Fig. 1 we plot the wave functions of all even states which may be assigned as $(0, v_2, 0)$ for $7 \leqslant v_2 \leqslant 12$. These plots show cuts through the wave functions at $\theta = 90°$. At this angle, odd functions (with respect to θ) have zero amplitude, so we are restricted to plotting only even functions. The
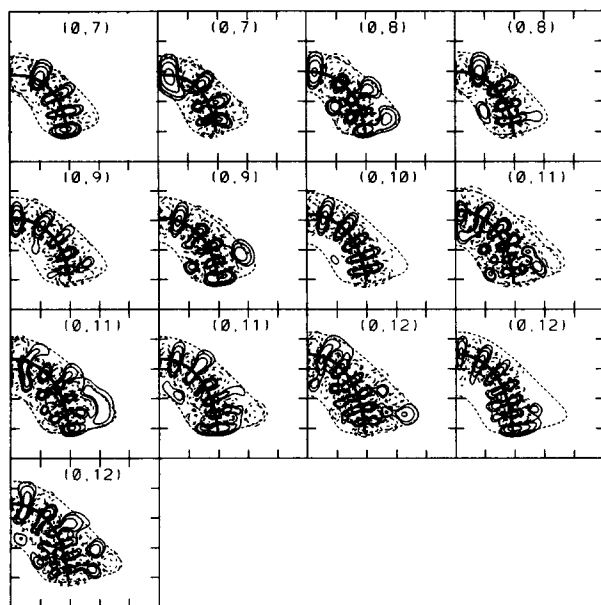
FIG. 1. 3D quantum mechanical horseshoe states on the MBB surface. The coordinates are mass weighted Jacobi coordinates, defined as $\tilde{r} = \alpha r$, $\tilde{R} = R/\alpha$, $\alpha = (3/4)^{1/4}$. R,r are the x,y coordinates, respectively. Each tic mark on the figures is 1 a.u. The numbers in parentheses denote the quantum numbers (ν_1, ν_2), respectively. $\nu_3 = 0$ for all states. The heavy solid lines show the quantized horseshoe periodic orbits for each state.

value of ν_2 is defined as the number of nodes of any given state along the horseshoe mode for positive values of the Jacobi coordinate R.

In Fig. 2 we plot the even wave functions of all states which have one or more excitations along the symmetric stretch. Although excited states can be assigned, it is clear that they become fewer as the ν_1 quantum number increases. This is reminiscent of a similar analysis of resonances in the reactive scattering of $H + H_2$ (Ref. 19), where the number
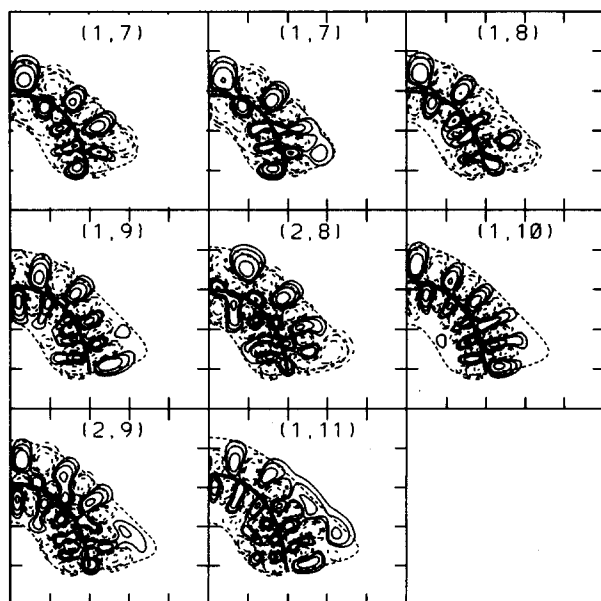
of observed excitations along the bending mode of the resonance is limited. The energies of all states shown in Figs. 1 and 2 are given in Table I.

By analyzing the states along the angle of 90°, one does not gain any information on the "antisymmetric stretch" quantum number ν_3 associated with these states. One only knows that it must be an even number. More information may be obtained by studying cuts of the wave functions at different values of θ, as shown in Fig. 3, for the (0,12,0) state on the DIM potential energy surface. The striking result is that the basic structure of the states in Fig. 3 is unchanged, indicating that all these states may indeed be assigned as $\nu_3 = 0$. We were not able to identify states with $\nu_3 \geqslant 2$.

Having established the assignment, we note from Figs. 1 and 2 that it is not single valued. More than one eigenstate can seemingly be assigned by the same set of quantum numbers. This ambiguousness can stem from two sources. The threefold permutation symmetry of the system can result in three (unsymmetrical) states with the same approximate quantum numbers. This seems, though, not to be a sufficient explanation for the five "horseshoe states" assigned as (0,17,0) (see Fig. 4). This result may be interpreted within the framework of the Feshbach resonance theory. The horseshoe orbit identifies a region of space which is relatively decoupled. This leads to a local set of states. However, this local set interacts with the background so that a given local state may have a prominent amplitude in more than one exact eigenstate. The range of energy spanned by all "degenerate" states assigned with the same set of quantum numbers can be interpreted as the width of the localized state as would be found in a stabilization computation. Thus, this energy range gives an indication of the time scale for intramolecular vibrational redistribution associated with the local mode. We believe that the relatively large width is crucial in understanding the coarse-grained spectrum of H_3^+. This

FIG. 2. Symmetric stretch excitations of 3D quantum mechanical horseshoe states of the MBB potential. Other notation is as in Fig. 1.

TABLE I. Properties of assigned horseshoe states of the MBB potential. Energies are relative to the bottom of the well.

ν_1	ν_2	E_{3D} (cm^{-1})	E_{2D} (cm^{-1})	E_{zpe} (cm^{-1})
0	7	18 069.5	16 821.2	1248.3
0	8	19 425.5	18 429.7	995.8
0	8	19 467.3	18 429.7	1037.6
0	9	21 059.1	20 184.5	874.6
0	9	21 076.7	20 184.5	892.2
0	10	22 796.6	22 056.8	739.8
0	11	24 541.1	23 962.3	578.8
0	11	24 574.5	23 962.3	612.2
0	11	24 604.7	23 962.3	642.4
0	12	26 483.3	25 917.9	565.4
0	12	26 539.6	25 917.9	621.7
0	12	26 569.7	25 917.9	651.8
1	7	20 559.1	19 443.6	1115.5
1	7	20 607.3	19 443.6	1163.7
1	8	22 109.8	21 001.6	1108.2
1	9	23 442.9	22 716.2	726.7
1	10	25 217.8	24 514.2	703.6
1	11	26 980.5	26 428.1	552.4
2	8	24 454.0	23 525.2	928.8
2	9	25 992.8	$\cdots$	$\cdots$

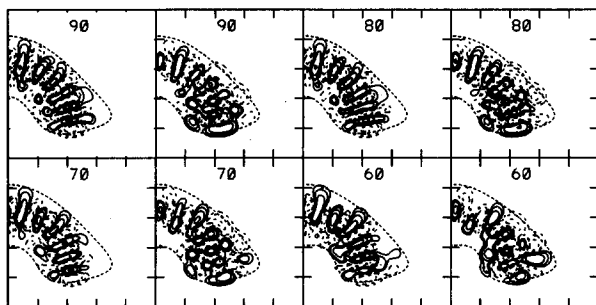FIG. 3. Angular dependence of a 3D horseshoe state. The state is (0,12,0) on the DIM potential energy surface. Both states having this assignment are shown. The number in each panel denotes the angle (in degrees).

will be further discussed in Sec. IV.

The observation that all states are in the ground anti-symmetric stretch mode makes it possible to use the assignment to estimate a zero point energy associated with this motion. In Ref. 10 we gave a detailed list of all C_{2v} states that are odd with respect to reflection (in the reduced space) around $R = 0$. When normalized such that
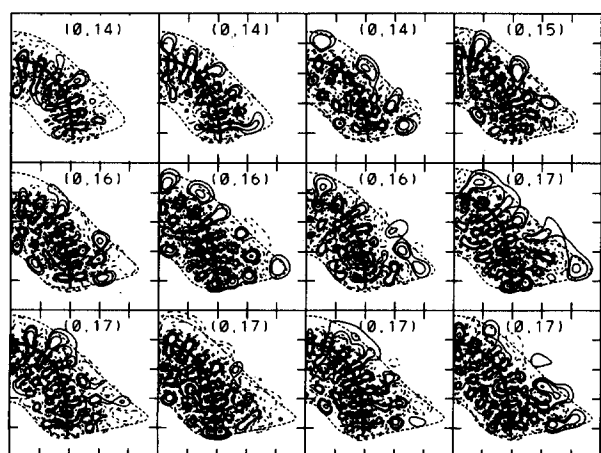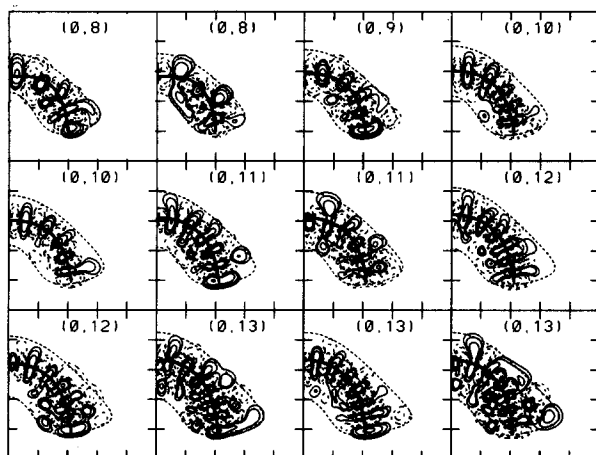
$$\iint dr\, dR\, |\psi_{C_{2v}}|^2 = 1,$$

FIG. 4. 3D quantum mechanical horseshoe states on the DIM potential. All notation is as in Fig. 1.

these states have a nodal line at $R = 0$. Note that all 3D states shown in Figs. 1–5 have nodal lines at $R = 0$. In the 3D case, the square root of the Jacobian factor R^2 has been included in the 3D wave functions so that these cuts may be compared directly with the similar plots obtained in the reduced dimension computations. As a result, the difference between the energy $E(v_1,v_2,0)$ of a 3D state and the energy $E(v_1,v_2)$ of the odd reduced dimension state is a measure of the zero point energy for the antisymmetric stretch mode. In Table I we give the relevant quantitative estimates. These will be compared in Sec. III with values obtained from a stability analysis of the horseshoe orbits.

In the reduced dimension computation one also finds states that are even with respect to reflection about $R = 0$. The numerical results of the 3D computation show that these states are disallowed at $J = 0$. In this paper we restricted ourselves to the $J = 0$ case since convergence at $J = 1$ was much more difficult, especially for the highly excited states.

C. DIM potential

The basis set used is large but not sufficient for converging all states of the DIM potential with spectroscopic accuracy. Altogether we studied 500 bound states. The energy of the 500th state is 36 684.4 cm^{-1} relative to the bottom of the H_3^+ well. This is 3028.7 cm^{-1} below the classical dissociation threshold into $H^+ + H_2$. The number 500 is only a lower bound to the true number of bound states up to this energy because of the poor convergence at high energies. Only the first 12 states are below the collinear threshold energy. For states lying below 25 000 cm^{-1} an accuracy of 10 cm^{-1} is obtained but we did not attempt to estimate the error in higher lying states. However, the basis set we are using covers the horseshoe region of the potential rather well, even at "high" energy. The spatial extent of horseshoe periodic orbits does not change dramatically with energy. It is plausible therefore to assume that even though many states are not converged at high energy, especially those with substantial amplitude leading to the asymptotic region, those states which can be characterized as horseshoe states will still remain reasonably well converged. This situation is
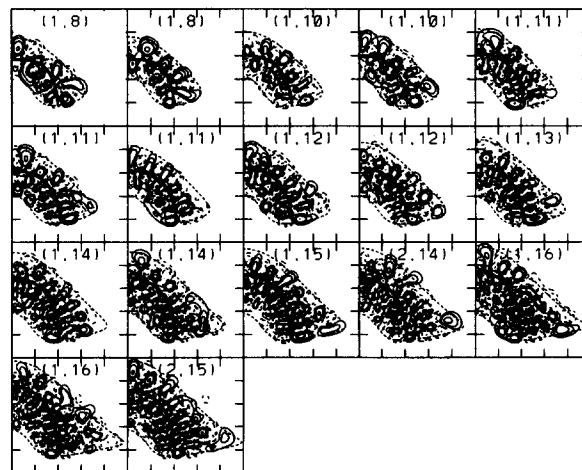

FIG. 5. Symmetric stretch excitations of 3D quantum mechanical horseshoe states of the DIM potential.

analogous to a stabilization calculation where one expects a change in the stabilization parameter to change the energies of spurious states only. Here, an increase in the basis set will mostly affect the background states but not the localized ones. A partial test of this assumption will be given in the next section where we show that the energies of the high lying localized states are in agreement with predictions of the periodic orbit quantization method.

All horseshoe states found with energy below the dissociation threshold, assigned as $(0,\nu_2,0)$ are shown in Fig. 4. Apart from the extention to much higher energies, this figure is very similar to Fig. 1 obtained for the MBB surface. As noted in previous classical[8] and quantal[10] studies, the horseshoe mode is quite insensitive to the details of the potential energy surface. The energies of all these states are given in Table II. Estimates for the antisymmetric stretch zero point energy, also given in the table, are based on the reduced dimension computations of Ref. 10 and estimated as described above for the MBB potential. Note that the incomplete convergence of the higher lying 3D states implies that these esti-

TABLE II. Properties of assigned horseshoe states of the DIM potential. Energies are relative to the bottom of the well.

ν_1	ν_2	E_{3D} (cm⁻¹)	E_{2D} (cm⁻¹)	E_{zpe} (cm⁻¹)
0	8	18 148.5	17 230.0	918.4
0	9	19 850.2	18 916.8	933.3
0	10	21 564.0	20 769.4	794.5
0	10	21 570.2	20 769.4	800.7
0	11	23 380.0	22 714.9	665.0
0	11	23 409.7	22 714.9	694.7
0	12	25 428.2	24 720.6	707.5
0	12	25 443.7	24 720.6	723.0
0	13	27 289.5	26 763.1	526.3
0	13	27 321.5	26 763.1	558.3
0	13	27 342.5	26 763.1	579.3
0	14	29 232.2	28 848.9	383.2
0	14	29 316.2	28 848.9	467.2
0	14	29 362.0	28 848.9	513.0
0	15	31 374.5	30 927.0	447.4
0	16	33 306.8	32 998.1	308.6
0	16	33 458.8	32 998.1	460.6
0	16	33 550.6	32 998.1	552.4
0	17	35 364.4	35 049.2	315.1
0	17	35 406.0	35 049.2	356.7
0	17	35 432.9	35 049.2	383.6
0	17	35 476.7	35 049.2	427.4
0	17	35 541.6	35 049.2	492.3
1	8	20 700.9	⋯	⋯
1	8	21 013.5	⋯	⋯
1	10	24 133.2	23 490.0	643.1
1	10	24 202.7	23 490.0	712.6
1	11	25 905.4	25 391.0	514.3
1	11	25 945.5	25 391.0	554.4
1	11	26 053.0	25 391.0	661.9
1	12	27 851.6	⋯	⋯
1	12	28 113.5	⋯	⋯
1	13	29 947.1	⋯	⋯
1	14	31 778.1	31 441.4	336.6
1	14	32 097.1	31 441.4	655.6
1	15	34 006.8	33 505.7	501.0
2	14	34 421.5	33 905.5	515.9
1	16	35 950.0	35 583.5	366.4
1	16	36 043.5	35 583.5	459.9
2	15	36 401.3	⋯	⋯

mates are actually only an upper bound.

In Fig. 5 we plot the even wave functions (with respect to θ) for all horseshoe states which can be assigned as having one or more excitations in the symmetric stretch mode. This is the DIM analogue of Fig. 2 for the MBB potential. Although qualitatively the results are similar, there are consistently less states on the DIM surface with higher ν_1 excitations. This is a further reflection of the fact that the DIM surface seems to be more "chaotic" leading to less localization. The overall correspondence of the two surfaces does indicate that the properties of the horseshoe mode are robust and should be expected to be important for any surface having the general topology and energetics of the H_3^+ molecule.

III. CLASSICAL ANALYSIS

A. 3D stability analysis

For zero total angular momentum, the classical Hamiltonian in the body-fixed coordinate system (using Jacobi coordinates) is

$$H = \frac{1}{2\mu_1} p_r^2 + \frac{1}{2\mu_2} p_R^2 + \frac{1}{2}\left(\frac{1}{\mu_1 r^2} + \frac{1}{\mu_2 R^2}\right) p_\theta^2 + V(r,R,\theta). \qquad (1)$$

The horseshoe orbit corresponds to motion in a T-shaped configuration so that the momentum (p_θ) conjugate to the angle θ is zero. Although the horseshoe orbit passes twice (within a period) through the collinear plane ($R = 0$), this does not lead to any divergence, since the momentum p_θ is zero along the orbit. However, for a stability analysis, one needs to consider the second derivatives of the Hamiltonian, where the singularity at $R = 0$ causes numerical instability.

To circumvent this problem we have followed a suggestion made by Nowotny and Schlier[20] and considered the full Hamiltonian in a space-fixed frame (cf. Fig. 6). Denote the three atoms as a,b,c, and their coordinates in a space-fixed frame as $\mathbf{q}_i$, $i = a,b,c$, respectively. The Lagrangian of the system is

$$L = \tfrac{1}{2} m_a \dot{\mathbf{q}}_a^2 + \tfrac{1}{2} m_b \dot{\mathbf{q}}_b^2 + \tfrac{1}{2} m_c \dot{\mathbf{q}}_c^2 - V(\mathbf{q}_a,\mathbf{q}_b,\mathbf{q}_c). \qquad (2)$$

Taking the origin of the coordinates system at the center of mass leads to the relation

$$-\mathbf{q}_c = (m_a \mathbf{q}_a + m_b \mathbf{q}_b)/m_c. \qquad (3)$$
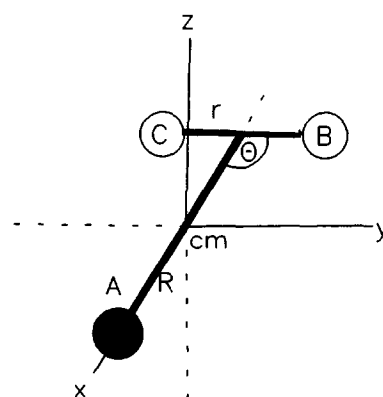

FIG. 6. Schematic diagram of the space-fixed coordinate system.

Linear momentum conservation gives the additional result

$$-\dot{\mathbf{q}}_c = \frac{1}{m_c} - (m_a \dot{\mathbf{q}}_a + m_b \dot{\mathbf{q}}_b),\tag{4}$$

so that the Lagrangian may be written in terms of the two vectors $\mathbf{q}_a$ and $\mathbf{q}_b$:

$$L = \frac{1}{2} m_a \dot{\mathbf{q}}_a^2 + \frac{1}{2} m_b \dot{\mathbf{q}}_b^2 + \frac{1}{2m_c} (m_a \dot{\mathbf{q}}_a + m_b \dot{\mathbf{q}}_b)^2 - V.\tag{5}$$

Using standard techniques[21] one finds the Hamiltonian in terms of these two vectors and their conjugate momenta:

$$H = \frac{1}{2M} \left(\frac{m_b + m_c}{m_a} \mathbf{p}_a^2 + \frac{m_a + m_b}{m_c} \mathbf{p}_b^2 - 2\mathbf{p}_a \mathbf{p}_b \right) + V.\tag{6}$$

The Liapunov stability analysis[22] of the horseshoe orbit proceeds now in two steps. The first consists of locating the orbit, using the reduced (two degrees of freedom) C_{2v} Hamiltonian in body-fixed coordinates [$p_\theta = 0$, $\theta = \pi/2$ in Eq. (1)]. This search is done in standard form, using the turning point method described in Ref. 23. One finds with high accuracy an initial set of points on the orbit and its period. It is convenient to choose the initial set on the equipotential line, such that the momenta are zero.

The results of the reduced dimension computation are then used as input for the stability analysis in the space-fixed frame. The orientation of the space-fixed frame is chosen such that the orbit lies in the x–y plane ($z = 0$) with the body-fixed R axis along the space-fixed x axis (cf. Fig. 6). It is now straightforward to numerically integrate the equations of motion in the space-fixed frame. For the Liapunov stability analysis one has, after one period, a matrix whose dimension is 12×12, leading to six pairs of eigenvalues, such that the product of each pair is one. Of the six distinct eigenvalues, three are equal to one because of conservation of total angular momentum. The eigenvectors are distinct and identical to the principal moments of inertia of the molecule. One additional pair has a value of one, and is associated with energy conservation. This leaves us with two distinct pairs, one is associated with the symmetric (v_1) mode. This eigenvalue is also identified by inspecting the eigenvector. We find that it is identical to the eigenvalue obtained from a stability analysis performed in the restricted C_{2v} problem. The remaining pair is similarly identified as associated with the antisymmetric stretch (v_3) motion.

The stability analysis in the reduced C_{2v} subspace has been carried out previously in Ref. 10. We found that at all relevant energies on the MBB and DIM surfaces, the horseshoe orbit was stable. The eigenvalues and absolute stability frequencies for the v_1 mode may be found in Table V of Ref. 10 and are also provided in Table III. The quantum number v_2 is determined by semiclassical quantization of the motion along the orbit. As mentioned in the previous section, for

TABLE III. Properties of the horseshoe orbit. Energies are relative to the bottom of the well of each surface, respectively. The collinear threshold is 14 275.53 (12 347.33) cm^{-1} for the MBB (DIM) surface. The dissociation energy to $H_2 + H^+$ is 39 713.08 cm^{-1} on the DIM surface. The notation $\Delta\omega_{v_2}^i$, $i = 1,3$ refers to the relative stability frequency [cf. Eqs. (7) and (8)] of the ith mode for the horseshoe orbit whose bending quantum number is v_2. $\omega_{v_2}^i$ is the absolute frequency.

n_2	Energy (cm^{-1})	$\Delta\omega_{v_2}^1$ (cm^{-1})	$\omega_{v_2}^1$ (cm^{-1})	$\omega_{v_2}^2$ (cm^{-1})	$\Delta\omega_{v_2}^3$ (cm^{-1})	$\omega_{v_2}^3$ (cm^{-1})
	MBB					
7	15 502.44	i353.53	2605.49	750.653	141.27	$\cdots$
8	17 117.86	i30.12	2591.20	853.693	i226.38	1933.77
9	18 890.78	i142.63	2602.08	914.903	195.73	$\cdots$
10	20 762.33	i285.88	2574.55	953.478	i328.78	1578.18
11	22 693.43	i364.46	2561.89	975.118	i373.62	1348.74
12	24 653.76	i391.93	2558.09	983.340	i143.90	1127.24
13	26 620.13	i384.77	2560.23	981.683	180.78	$\cdots$
14	28 576.14	i358.26	2561.93	973.396	223.14	$\cdots$
	DIM					
8	15 727.36	i372.91	2907.90	844.998	i216.39	1906.39
9	17 496.29	i87.22	2835.59	916.123	236.60	$\cdots$
10	19 378.03	i97.10	2796.42	964.508	i294.20	1634.82
11	21 343.68	i240.24	2758.70	999.647	i378.51	1378.09
12	23 368.77	i343.69	2727.83	1023.839	110.30	$\cdots$
13	25 433.03	i408.87	2705.94	1038.271	293.10	$\cdots$
14	27 515.92	i438.09	2692.93	1043.674	327.87	$\cdots$
15	29 601.36	i438.27	2685.77	1041.345	311.63	$\cdots$
16	31 676.98	i418.78	2680.15	1032.975	261.29	875 ± 66^a
17	33 730.90	i387.76	2672.88	1020.214	170.11	875 ± 66^a
18	35 755.81	i350.63	2662.45	1004.360	i129.96	874.40
19	37 747.16	i310.40	2648.62	986.340	i260.08	726.26
20	39 700.31	i268.49	2631.90	966.795	i351.09	615.71
21	41 613.37	i225.15	2613.32	946.157	i430.24	515.92
22	43 484.17	i179.55	2594.65	924.733	i418.23	506.50
23	45 311.59	i128.68	2579.52	902.734	i314.76	587.97
24	47 094.52	i58.30	2582.65	880.318	i187.17	693.15

^{a} These are estimates for the adiabatic frequencies for energies at which the orbit is unstable.

$J = 0$ all states have a nodal line at $R = 0$. Thus, the semi-classical quantization condition for the action is $(2v_2 + 3/2)\hbar$.

The stability properties of the v_3 mode are given in Table III. Denote the eigenvalue as $\lambda_{v_2}^3$ and the period of the orbit as T_{v_2}. When the orbit is stable, the relative stability frequency $\Delta\omega_{v_2}^3$ is defined as

$$\Delta\omega_{v_2}^3 \equiv \frac{1}{iT_{v_2}}\ln\lambda_{v_2}^3. \tag{7}$$

When the orbit is unstable, the stability frequency is defined as

$$\Delta\omega_{v_2}^3 = \frac{1}{T_{v_2}}|\ln\lambda_{v_2}^3|. \tag{8}$$

In Fig. 7 we plot the relative stability frequencies for the v_3 mode and the two potential energy surfaces as a function of energy. As already observed qualitatively in Ref. 8(b), the orbit goes through cycles of stability and instability. The qualitative behavior is the same for both potential energy surfaces. It is important to note that the region of stability increases with energy and is quite large around the dissociation energy. As mentioned in the previous section, the quantum states of both surfaces localize around the horseshoe orbit even when it is unstable.

B. Stability frequency

When the periodic orbit is stable, the Liapunov stability analysis gives an eigenvalue whose exponent is defined up to $\mathrm{mod}(2\pi)$. The periodic orbit quantization method needs the physical frequency for the motion along the relevant mode as input. In a two degree of freedom system this is found by a variety of means; the easiest to implement is to follow the motion of a trajectory initiated close to the periodic orbit.[10] The number of times the adjacent trajectory crosses the peri-
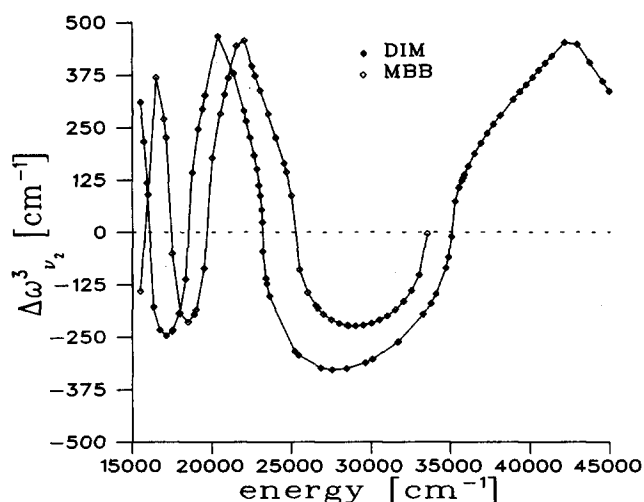

FIG. 7. Relative stability frequencies for the antisymmetric stretch mode of the horseshoe orbit. The stable regions are denoted with positive values of $\Delta\omega_{v_2}^3$ [cf. Eq. (7)]. In the unstable regions we give a negative value to the frequency so as to give a clear picture. The shift between the MBB and DIM results is due to the small differences in the energetics of the two surfaces. The energy scale is relative to the bottom of the H_3^+ well.
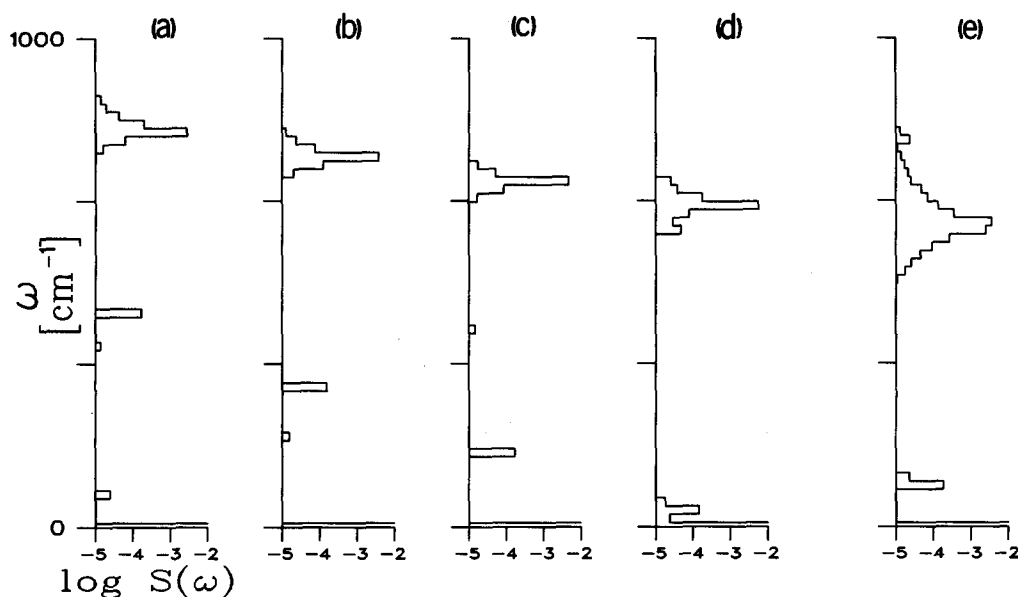
odic orbit reveals the absolute frequency. In a 3D problem, this procedure can no longer be implemented. The higher dimensionality causes the number of crossings to be ill defined; it depends on the coordinate system. Alternatively, we have used continuity to establish the absolute phase,[11] since at the bottom of a well the stability frequency of an orbit coincides with the harmonic frequency. In the case of the horseshoe orbit, at threshold, it is already highly nonlinear and the stability analysis cannot be approximated with a simple harmonic estimate. In addition, the rapid alternating regions of stability and instability close to threshold render it difficult to implement.

The analysis presented above, though, has established that of the two distinct eigenvalues, the v_1 mode is relatively stable. The stability frequency changes by $\sim 10\%$ over the whole energy region up to dissociation. This is clearly not the case for the v_3 mode. Consider then a power spectrum of trajectories initiated in the vicinity of the orbit. In principle, such a spectrum should have three fundamentals and their overtones. These are the v_1 and v_3 frequencies and the frequency of the orbit itself (v_2). If one now changes the energy somewhat, the v_1 and v_2 peaks will remain practically constant while the v_3 frequency will vary substantially. In this form one can identify the absolute value of the v_3 frequency.

In Fig. 8 we show spectra on the DIM surface in the energy range $-0.4 \leqslant E \leqslant 0$ eV (which is $36\,486 \leqslant E \leqslant 39\,713$ cm^{-1} relative to the bottom of the H_3^+ well). At -0.58 eV the orbit becomes stable and stays that way up to an energy of 1.23 eV above the dissociation threshold. These spectra are obtained by running the horseshoe orbit and an adjacent trajectory for a long time. The difference vector $[\Delta\mathbf{q}(t),\Delta\mathbf{p}(t)]$ is projected onto the difference vector at time $t = 0$. Figure 8 shows the power spectrum $S(\omega)$ of this projection, where the initial difference is a slight perturbation of the angle θ away from 90°. This choice is guided by the fact that the antisymmetric stretch motion must involve a change of angle.

One notes a peak that shifts considerably with energy. It is therefore identified as the v_3 frequency. To verify that the peak is the fundamental and not an overtone or combination we show in Fig. 9 the time dependence of the variable $\{[\Delta\mathbf{q}(0), \Delta\mathbf{p}(0)]\cdot[\Delta\mathbf{q}(t),\Delta\mathbf{p}(t)]\}$ (denoted sp in the figure) from which the period associated with the the v_3 peak can be discerned. Having established the absolute frequency of the v_3 motion at one energy, we use the results of the stability analysis to determine the frequency at all energies. Note that the absolute frequency remains the same as one goes through a cycle of instability. In this form we obtained $\omega_{v_2}^3$ for the whole range in which the orbit is stable.

In Fig. 10 we compare the classical results with the quantum frequencies obtained from the 2D and 3D quantum results as described in Sec. II B. The agreement is good. In Table IV we compare quantum energies predicted by the periodic orbit quantization formula:

$$E_{v_1,v_2,v_3} = E_{v_2} + (v_1 + 1/2)\hbar\omega_{v_2}^1 + (v_3 + 1/2)\hbar\omega_{v_2}^3 \tag{9}$$

and the exact quantum results. What is still lacking is an estimate of the v_3 adiabatic frequency in the energy range

FIG. 8. Power spectra $S(\omega)$ of slight angular perturbation of the horseshoe orbit. Panels a–e show the spectra at energies of -0.4, -0.3, -0.2, -0.1, and 0 eV relative to the classical $H^+ + H_2$ dissociation threshold (which corresponds to energies of 36 486.9, 37 293.4, 38 100.0, 38 906.5, and 39 713.1 cm^{-1} relative to the bottom of the H_3^+ well). At the lowest energy, the orbit is marginally stable and the v_3 peak is at the v_2 frequency. As energy is increased, the v_3 frequency decreases noticeably. For further details, see the text.

where the orbit is unstable. This is described in the next subsection.

C. Adiabatic frequency

The quantum localization even in the region where the periodic orbit is unstable in the sense of Liapunov implies that the orbit is still adiabatically stable. In other words, for short times, a trajectory initiated in the vicinity of the orbit will oscillate around it before moving away. Quantum mechanics are sensitive to the short time classical dynamics, as has been amply demonstrated for the resonances in atom-diatom reactive scattering.[23] In $H + H_2$ for example, the quantum resonances were shown to be associated with an unstable periodic orbit which was adiabatically stable. Similarly, for a quartic potential it has been recently demonstrated[17,24] that quantum localization occurs around an adiabatically stable orbit, which is unstable in the Liapunov sense.
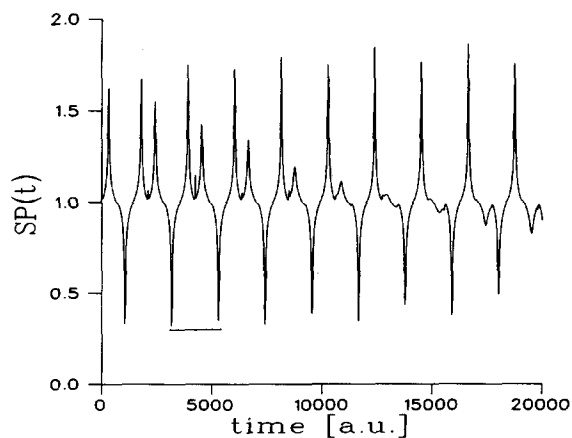

FIG. 9. Correlation function of the perturbed horseshoe spectrum, shown in Fig. 8 at $E = -0.1$ eV. Note the period of 2120 a.u. corresponding to a frequency of 650 ± 3 cm^{-1}. The horizontal brace indicates one period, sp is the scalar product, defined in the text.

The periodic orbit quantization formula gave a good estimate for the localized quantum states.[17]

In this subsection, we will demonstrate that the horseshoe orbit is adiabatically stable. An estimate of the adiabatic frequency will also be given in the region where the instability of the orbit is not too large. As indicated, the adiabatic frequency should be observable in the short time dynamics. In Fig. 11 we plot short time averaged spectra. The dynamical variable is the same as in Fig. 8. The main difference is that instead of integrating a single trajectory for a long time, we integrate 1000 trajectories initiated close to the orbit, but with angles slightly off 90° for short times. The integration time is limited by the instability of the orbit and the numerical accuracy in choosing the initial condition. We found it necessary to initiate trajectories distributed randomly over an initial distance $1 \times 10^{-6} \leqslant d(0) \leqslant 2 \times 10^{-6}$ a.u. For a given Liapunov eigenvalue $\lambda_{v_2}^3$, this implies that

$$d(t) = d(0)(\lambda_{v_2}^3)^{t/T_{v_2}}. \tag{10}$$

When the distance $d(t)$ is greater than 0.4 a.u., the orbit can no longer be thought of as being in the vicinity of the orbit and therefore will no longer give information on the adiabatic frequency. As a result we were able to get meaningful spectra with reasonable resolution provided that the stability frequency of the unstable orbit was not greater than 260 cm^{-1}.

Inspection of Fig. 11 shows a large peak at the frequency of the orbit (v_2), but also a second peak at a slightly lower frequency. It is this lower peak which may be identified as the adiabatic frequency, which is also used in Fig. 10 to compare with the quantum adiabatic results.

At the boundary between the stable and unstable regions, it has been shown in Ref. 18 that the adiabatic frequency and the stability frequency coincide. From Fig. 10, it would then seem that at the boundary, the classical results go through a minimum or a maximum while the quantum results are on the average a monotonically decreasing func-
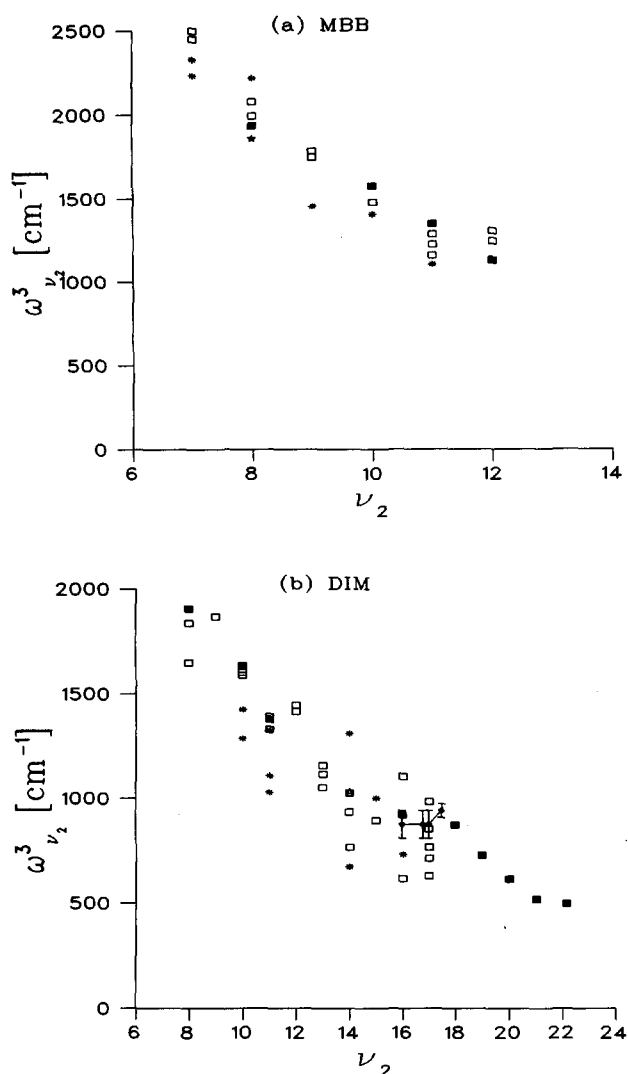
FIG. 10. Comparison of classical and quantum mechanical estimates of the v_3 frequency. The notation (open boxes, *, and stars) gives the quantum estimates for states assigned as $(0,v_2,0)$, $(1,v_2,0)$, and $(2,v_2,0)$ respectively. The closed boxes are the classical estimates, in the stable regions of the horseshoe. The closed diamonds (with error bars) are the classical estimate of the adiabatic frequency in a region where the orbit is unstable. Panels a, b are for the MBB and DIM potentials, respectively.

TABLE IV. Comparison of the quantal energies of Tables I and II and the semiclassical estimate [cf. Eq. (9)].

v_1	v_2	E_{qm} (cm^{-1})	E_{sc} (cm^{-1})
MBB			
0	8	19 467.3	19 380.4
0	10	22 796.6	22 838.7
0	11	24 541.1	24 648.7
0	11	24 574.5	24 648.7
0	11	24 604.7	24 648.7
0	12	26 483.3	26 496.4
0	12	26 539.6	26 496.4
0	12	26 569.7	26 496.4
1	8	22 109.8	22 938.4
1	10	25 217.8	25 413.3
1	11	26 980.5	27 210.6
2	8	24 454.0	25 529.6
DIM			
0	8	18 148.5	18 134.5
0	10	21 564.0	21 593.7
0	10	21 570.2	21 593.7
0	11	23 380.0	23 412.1
0	11	23 409.7	23 412.1
0	16	33 306.8	33 454.6[a]
0	16	33 458.8	33 454.6[a]
0	16	33 550.6	33 454.6[a]
0	17	35 364.4	35 504.84[a]
0	17	35 406.0	35 504.84[a]
0	17	35 432.9	35 504.84[a]
0	17	35 476.7	35 504.84[a]
0	17	35 541.6	35 504.84[a]
1	8	20 700.9	21 042.4
1	8	21 013.5	21 042.4
1	11	25 905.4	26 170.8
1	11	25 945.5	26 170.8
1	11	26 053.0	26 170.8

[a] These are based on the adiabatic frequencies, cf. Table III.

tion. This plot is similar to the quantum smoothing of classical mechanical divergences in differential cross sections. The quantum results are not sensitive to the fine details of the classical dynamics.

IV. DISCUSSION

The numerical results presented in this paper lead to the following conclusions which are of importance for analysis of the experimental coarse grained photodissociation spectrum of H_3^+:

(a) Quantum localizations are found around the horseshoe orbit even in 3D. These include states with excitations in the v_1 mode. No excitations in the v_3 mode could be observed.

(b) The horseshoe orbit changes stability with respect to the v_3 mode as a function of energy.

(c) Quantum localization occurs even in regions where the orbit is unstable.

(d) The localized quantum states can be assigned, using the periodic orbit quantization method.
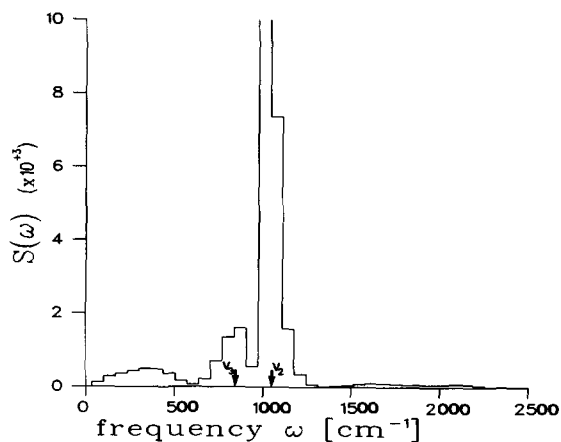

FIG. 11. Short time, averaged spectrum. The energy is that of the $v_2 = 17$ horseshoe orbit. Note the large peak at the v_2 frequency. The amplitude of this peak goes beyond the scale of the vertical axis, reaching an amplitude of 5.81×10^4. The adjacent broader peak shows the v_3 adiabatic frequency. The surface is DIM; for further details, see the text.

(e) The assignment is not unique, usually at least a couple of adjacent states split by ~ 50 cm^{-1} are assigned by the same set of periodic orbit quantum numbers.

(f) The v_3 frequency at the threshold for dissociation is determined from the stability analysis to be 638 ± 3 cm^{-1}, in good agreement with a previous estimate of 643 cm^{-1},[8(b)] based on classical dipole spectra.

The coarse-grained experimental photodissociation spectrum of H_3^+ has been assigned in Ref. 8(b) in terms of the R branch associated with the antisymmetric stretch frequency of the horseshoe orbit. The results of the present study are consistent with this interpretation. We have demonstrated that quantum states localize around the horseshoe orbit and that the quantum mechanical v_3 frequency is in good agreement with the classical estimate. This work is therefore an additional step in verification of the proposed assignment. There are, though, a number of questions which have yet to be answered. (1) For an R branch transition to be possible, one must demonstrate the existence of localized horseshoe states with one excitation in the v_3 mode. Such a state necessarily is odd with respect to reflection about $\theta = 90°$ and so was not observed in the present work. We have found states that localize with more than one excitation in the v_1 mode, even in regions where the classical regular phase space around the orbit is much too small to justify the localization. It is therefore plausible that excitations in the antisymmetric stretch mode also will exist, especially at the experimental energy range where the horseshoe orbit is stable. (2) As discussed in detail in Ref. 8(b), the experimental energy window for dissociating states at a given J is small. For the horseshoe ladder of states to be observable, it is necessary that this ladder covers the whole energy range. In the present study we have seen that a given horseshoe assignment is not unique and that typically two or three states have the same assignment. In terms of the Feshbach picture, the horseshoe state seems to be quite a broad resonance. This lends further credibility to the proposed assignment of the experimental spectrum. The present computation is, however, limited to $J = 0$ and it is necessary to study this property at $J = 5$, the experimentally accessible region. (3) The present study stresses the need for an accurate surface up to the dissociation energy and beyond.

It is clear that to verify the predicted assignment, it is necessary to compute the exact quantum spectrum. This should prove possible at least for transitions involving $J = 0$ and $J = 1$ which are somewhat below the dissociation threshold. The present study as well as the previous ones imply that as far as the coarse-grained spectrum is concerned, it is only weakly dependent on energy, justifying the very large computational effort involved.

ACKNOWLEDGMENTS

[1] E. Abramson, R. W. Field, D. Imre, K. K. Innes, and J. L. Kinsey, J. Chem. Phys. **83**, 453 (1985).

[2] M. Broyer, G. Delacretaz, G.-Q. Ni, R. L. Whetten, J.-P. Wolf, and L. Wöste, J. Chem. Phys. **90**, 4620 (1989).

[3] A. Carrington and R. M. Kennedy, J. Chem. Phys. **81**, 91 (1984); A. Carrington and I. R. McNab, Acc. Chem. Res. **22**, 218 (1989).

[4] D. E. Freeman, K. Yoshino, J. R. Esmond, and W. H. Parkinson, Planet. Space Sci. **32**, 239 (1984).

[5] J. M. Gomez Llorente, H. S. Taylor, and E. Pollak, Phys. Rev. Lett. **62**, 2096 (1989); J. M. Gomez Llorente and H. S. Taylor, J. Chem. Phys. **91**, 954 (1989).

[6] B. R. Johnson and J. L. Kinsey, Phys. Rev. Lett. **62**, 1607 (1989); J. Chem. Phys.

[7] M. Berblinger, E. Pollak, and Ch. Schlier, J. Chem. Phys. **88**, 5643 (1988).

[8] J. M. Gomez Llorente and E. Pollak, J. Chem. Phys. **89**, 1195 (1988); J. M. Gomez Llorente and E. Pollak, J. Chem. Phys. **90**, 5406 (1989).

[9] H. S. Taylor and J. Zakrzewski, Phys. Rev. A **38**, 3732 (1988); J. M. Gomez Llorente, J. Zakrzewski, H. S. Taylor, and K. C. Kulander, J. Chem. Phys. **90**, 1505 (1989).

[10] J. Tennyson, O. Brass, and E. Pollak, J. Chem. Phys. (in press).

[11] K. Stefanski and E. Pollak, Chem. Phys. **134**, 37 (1989); K. Stefanski and E. Pollak, J. Chem. Phys. **87**, 1079 (1987).

[12] R. M. Whitnell and J. C. Light, J. Chem. Phys. **89**, 3674 (1988); **90**, 1774 (1989).

[13] Z. Bacic and J. C. Light, Annu. Rev. Phys. Chem.

[14] J. Tennyson and J. R. Henderson, J. Chem. Phys. **91**, 3815 (1989).

[15] W. Meyer, P. Botschwina, and P. G. Burton, J. Chem. Phys. **84**, 891 (1986).

[16] R. K. Preston and J. C. Tully, J. Chem. Phys. **54**, 4297 (1971).

[17] B. Eckhardt, G. Hose, and E. Pollak, Phys. Rev. A **39**, 3776 (1989).

[18] E. Pollak, Chem. Phys. **61**, 305 (1981).

[19] E. Pollak, J. Phys. Chem. **90**, 3619 (1986).

[20] Ch. Schlier (private communication).

[21] H. Goldstein, *Classical Mechanics* (Addison–Wesley, Reading, MA, 1950).

[22] N. Minorsky, *Nonlinear Oscillations* (Van Nostrand Reinhold, Princeton, NJ, 1962), Ch. 5.

[23] E. Pollak, in *Theory of Chemical Reaction Dynamics*, edited by M. Baer (CRC, Boca Raton, FL, 1985), Vol. 3, p. 123, and references therein.

[24] C. C. Martens, R. L. Waterland, and W. P. Reinhardt, J. Chem. Phys. **90**, 2328 (1989).